

HARD X-RAYS FROM SN 1993J

M. D. LEISING,¹ J. D. KURFESS,² D. D. CLAYTON,¹ D. A. GRABELSKY,³ J. E. GROVE,² W. N. JOHNSON,²
 G. V. JUNG,⁴ R. L. KINZER,² R. A. KROEGER,² W. R. PURCELL,³ M. S. STRICKMAN,²
 L.-S. THE,¹ AND M. P. ULMER³

Received 1994 March 4; accepted 1994 June 9

ABSTRACT

The Oriented Scintillation Spectrometer Experiment (OSSE) on the *Compton Observatory* observed SN 1993J during three intervals centered approximately 12, 30, and 108 days after its outburst. Hard X-ray emission was detected in the first two of these intervals. No emission was seen in the third observation or in two earlier observations in 1991 and 1992. The coincidence of the observed excess with the outburst of SN 1993J and the consistency of the spectra and time evolution with those seen at lower energies by *ROSAT* and *ASCA* (*Astro-D*) argue that the observed emission is indeed from SN 1993J. It is probably due to the interaction of the fast supernova ejecta with circumstellar material. The luminosity, 5×10^{40} ergs s⁻¹ (50–150 keV) in the first interval, is significantly larger than predicted. Extrapolating the spectrum to a few keV accounts for most or all of the observed emission at low energy. The observed high temperature, 10⁹ K, is easily obtained in the shocked circumstellar matter, but a surprisingly high density is required there to give the observed luminosity, and little or no additional X-ray emission from denser shocked supernova ejecta is allowed. The hard emission might also be explained in terms of the shocked supernova ejecta itself with unexpectedly high temperature.

Subject headings: circumstellar matter — gamma rays: observations — supernovae: individual (SN 1993J) — X-rays: general

1. INTRODUCTION

The great potential of hard photon diagnostics of supernovae has been well documented. The quantity and location of radioactivity, the nature of the interaction of the fast ejecta with external material, and the presence and character of a compact remnant can all be addressed with X-ray and γ -ray observations. Indeed, some of this potential was realized from observations of SN 1987A (Sunyaev et al. 1987; Dotani et al. 1987; Matz et al. 1988). In that case the hard X-ray emission, as well as the γ -ray line emission, can be understood as arising from decay of radioactive ⁵⁶Co within the ejecta. SN 1980K was also detected in soft X-rays (Canizares, Kriss, & Feigelson 1982) that were probably produced by the interaction of the ejecta with circumstellar material. Whether this emission was of thermal or nonthermal origin could not be determined.

SN 1993J in NGC 3031 (M81) has been extensively observed at many wavelengths and has yielded a wealth of new information about core collapse supernovae (Wheeler & Filippenko 1994, and references therein). It is a transition object, appearing initially with Type II supernova spectral characteristics and then evolving into a Type Ib object (Filippenko, Matheson, & Ho 1993; Swartz et al. 1993). The light curve was also quite unusual (Schmidt et al. 1993). The observed characteristics are well modeled as the result of a core collapse and subsequent explosion in a red supergiant that had lost almost all of its hydrogen-rich envelope (Nomoto et al. 1993; Podsad-

lowski et al. 1993; Wheeler et al. 1993; Schmidt et al. 1993; Hoflich, Langer, & Duschinger 1993; Woosley et al. 1994), probably due to interactions with a binary companion.

Soft X-rays were detected from SN 1993J beginning only 6 days after the explosion, and subsequent X-ray observations showed a slowly declining flux, with decay timescales of a few months (Zimmermann et al. 1994; Tanaka 1993). All X-ray spectra were quite flat, with photon power-law indices near -1.0. For thermal spectral models, only lower limits on the electron temperature, near $kT_e = 10$ keV, could be established. These data have been interpreted in terms of thermal bremsstrahlung emission from shock-heated electrons due to the interaction of the expanding supernova ejecta with circumstellar material, presumably the presupernova stellar wind (Suzuki et al. 1993; Chevalier & Fransson 1994). In principle, significant X-ray emission can come from both the wind material shocked to high temperatures ($\sim 10^9$ K) just ahead of the ejecta (Fransson 1984), and from the ejecta (Chevalier 1982) if the overpressure resulting from the primary shock drives a “reverse” shock into the ejecta (McKee 1974). Despite the lower temperature in the shocked ejecta, it could dominate the soft X-ray luminosity because of its higher free-free emissivity due to its higher density. Hard X-ray observations are required to assess the contribution of the shocked wind itself and better to constrain the electron temperature, if the emission is indeed thermal. Combined hard and soft X-ray measurements can in principle distinguish between thermal and nonthermal emission mechanisms. Early detections of radio emission from SN 1993J also imply circumstellar interactions (Pooley & Green 1993; Van Dyk et al. 1993; Phillips & Kulkarni 1993).

2. OBSERVATIONS AND DATA ANALYSIS

The Oriented Scintillation Spectrometer Experiment (OSSE) is one of four experiments on NASA’s *Compton Gamma-Ray*

¹ Department of Physics and Astronomy, Clemson University, Clemson, SC 29634-1911. E-mail: leising@gamma.phys.clemson.edu.

² E. O. Hulburt Center for Space Research, Naval Research Laboratory, Washington, DC 20375-5320.

³ Department of Physics and Astronomy, Northwestern University, Evanston, IL 60201.

⁴ Universities Space Research Association, Washington, DC 20024.

Observatory satellite (Johnson et al. 1993). OSSE was designed to undertake observations of astrophysical sources in the 0.05–10 MeV range. It consists of four identical detector systems with independent, single-axis orientation controls that provide a range of 192° . The primary detecting element for each detector is a large-area NaI(Tl) scintillation crystal (13 inches [33 cm] diameter by 4 inches [10 cm] thick) shielded in the rear by an optically coupled 3 inch (7.6 cm) thick CsI(Na) scintillation crystal in a “phoswich” configuration. Each phoswich is actively shielded by a 3.3 inch (8 cm) thick annulus of NaI(Tl) scintillation crystals and passively collimated by a tungsten slat collimator that defines a 3.8×11.4 full width at half-maximum (FWHM) γ -ray aperture. The total aperture area of the four detectors is 2620 cm^2 , with an effective photopeak area of 2000 cm^2 at 511 keV.

Shortly after the discovery of SN 1993J the nature of the explosion was unclear. Mainly in view of the possibility of early leakage of ^{56}Ni γ -rays, the *Compton Observatory* was reoriented to observe the supernova as soon as possible. A 6 day observation was followed by a full 2 week observation after 8 intervening days. These two observations are the main focus of this work. Later, when the probability of detecting ^{56}Co γ -rays was near maximum, OSSE observed SN 1993J for 4 weeks. The three observation intervals are summarized in Table 1. The accumulation times listed are total on-source times for four detectors. Comparable time was spent on background observations. Two previous observations, nominally of M82 but also including M81 in the field of view (they are separated by $\sim 1^\circ$), are also listed.

OSSE observations consist of a sequence of 2 minute observations of a source field alternated with 2 minute offset-pointed background measurements. The 2 minute duration is selected to be short relative to the typical orbital background variations. When possible, source-free fields 4.5° offset on both sides of the source position along the detector scan plane are used for background observations.

Data screening selected only the highest quality data of both source and background observations. Background estimation was achieved by performing a quadratic fit to three or (where possible) four 2 minute background accumulations within 6 minutes on either side of every 2 minute source accumulation. The interpolated background count rate spectrum is subtracted from each source spectrum. The differences are screened for anomalies and then averaged over times appropriate for spectral analysis. Spectra are characterized by defining a photon spectrum model, convolving the model with the instrument response function, comparing the resultant energy loss spectrum with the observed count rate spectrum, and varying the model parameters until the best agreement is

TABLE 1
SN 1993J/M81 OBSERVATION SUMMARY

CGRO Period	Dates	Days from Explosion ^a	Accumulation Time ^b (10^5 s)
216	1993 Apr 6–12	9.9–15.4	0.84
218	1993 Apr 20–May 3	23.7–36.9	1.49
227/228	1993 Jun 29–July 27	93.6–121.5	4.53
7	1991 Aug 9–15	...	0.80
18	1992 Jan 10–23	...	1.80

^a Taken to be 1993 March 28.0.

^b Total time of source observations with four detectors.

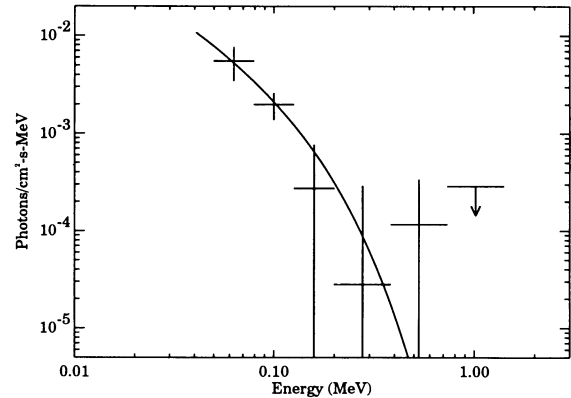


FIG. 1.—The SN 1993J photon spectrum observed by OSSE during the interval 9.9–15.4 days after the explosion (assumed March 28.0). Error bars are 1σ , and the upper limit is the 2σ limit. The solid line shows the best-fit thermal bremsstrahlung model used in the model-dependent deconvolution.

obtained. A detailed description of OSSE performance and spectral data analysis procedures can be found in Johnson et al. (1993).

3. RESULTS

The difference spectrum averaged over April 6–12 (days 9.9–15.4) shows a clear excess at energies $\leq 200 \text{ keV}$. The corresponding photon spectrum is shown in Figure 1. Also shown as the solid line is the best-fit thermal bremsstrahlung model used in the model-dependent deconvolution. The fit was performed with the full OSSE energy resolution and the reduced chi-squared $\chi^2 = 0.85$ for 159 degrees of freedom. The intensity at 100 keV is $2.11_{-0.45}^{+0.44} \times 10^{-3} \text{ cm}^{-2} \text{ s}^{-1} \text{ MeV}^{-1}$, and the temperature is $kT_e = 82_{-29}^{+61} \text{ keV}$. These uncertainties are “ 1σ ” values derived from unit increase in χ^2 with other parameters allowed to vary freely. More meaningful uncertainties are represented in Figure 2, where we show confidence level contours for the two-parameter fit. The electron temperature is very well constrained on the low side; the spectrum cannot cut off below

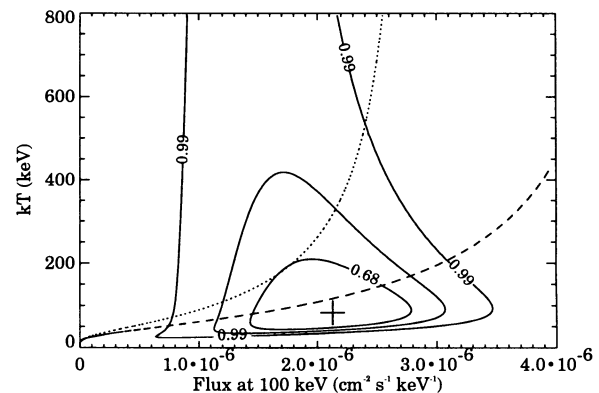


FIG. 2.—Confidence levels (68%, 90%, and 99%) for various values of the two parameters of the thermal bremsstrahlung model fitted to the OSSE spectrum from the interval 9.9–15.4 days. The cross shows the position of the best fit. The temperature is well constrained on only the low side. The dashed line shows the combinations of parameter values that extrapolate to the absorption corrected total flux observed from 0.1 to 2.4 keV by *ROSAT* on day 12 (Zimmermann et al. 1994). Similarly, the dotted line shows parameter combinations that agree with the reported *ASCA* total flux (1–10 keV) on day 8 (Tanaka 1993).

the OSSE energy range. However, very high temperatures are allowed. Thus we do not determine well the degree of equipartition between electrons and ions. Although it is not shown, even the contour corresponding to significance of 10^{-4} does not extend to zero flux; the contour of 3×10^{-5} just does. This statement best reflects the total statistical significance of the measurement.

A power-law model also fits equally well with $\chi^2_\nu = 0.86$. The best-fit power-law amplitude at 100 keV is $1.89^{+0.41}_{-0.42} \times 10^{-3} \text{ cm}^{-2} \text{ s}^{-1} \text{ MeV}^{-1}$, and the photon spectral index is $-2.24^{+0.46}_{-0.48}$. For this model the contour corresponding to significance 1×10^{-5} is the first to extend to zero flux. If the emission is attributed to SN 1993J, either model implies a very large X-ray luminosity, near $5.3 \times 10^{40} \text{ ergs s}^{-1}$ (50–150 keV) at distance 3.6 Mpc (Freedman et al. 1994).

The next observation, April 20–May 3, also exhibits some evidence, although statistically weak, for hard X-ray emission. The photon spectrum from this interval is shown in Figure 3, as is the best-fit thermal bremsstrahlung model. The fitted intensity at 100 keV is $9.4^{+3.6}_{-3.8} \times 10^{-4} \text{ cm}^{-2} \text{ s}^{-1} \text{ MeV}^{-1}$, with temperature $kT_e = 74^{+120}_{-40} \text{ keV}$, and $\chi^2_\nu = 1.02$ for 159 degrees of freedom. This is formally less intense than the previous observation, although we cannot rule out a constant spectrum over the two intervals.

In the last observation, June 29–July 27, we find no evidence for emission at any energy. Because of the long observation time, the upper limit on the hard X-ray flux is well below the previously observed values. We have also analyzed 1991 and 1992 observations, nominally of NGC 3034 (M82), because they also included M81 in their source fields (see also Bhattacharya et al. 1994). We find no evidence for emission from any object in the source fields at any energy during those two pre-SN 1993J observations. The measured 50–200 keV fluxes, derived using thermal bremsstrahlung fits, for all five observations are plotted in Figure 4.

4. DISCUSSION

Because of OSSE's large field of view and lack of imaging capability, we cannot with certainty attribute the excesses observed in the first two 1993 observations to SN 1993J. Both M82 and the nucleus of M81 are known X-ray sources and are in the OSSE source fields. However, the coincidence of the positive flux with the occurrence of SN 1993J is suggestive. Also, both *ROSAT* and *ASCA* definitely detected X-rays from

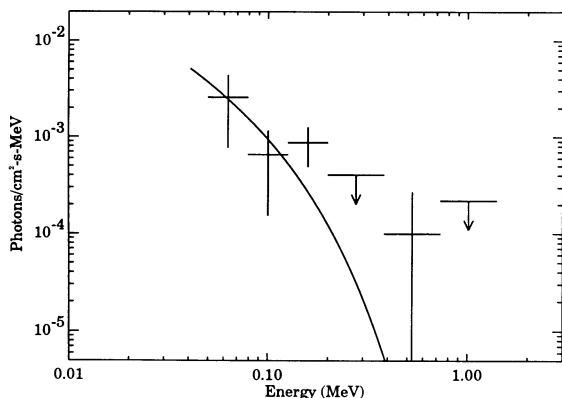


FIG. 3.—The SN 1993J photon spectrum observed by OSSE during the interval 23.7–37.0 days after the explosion (assumed March 28.0). The solid line shows the best-fit thermal bremsstrahlung model.

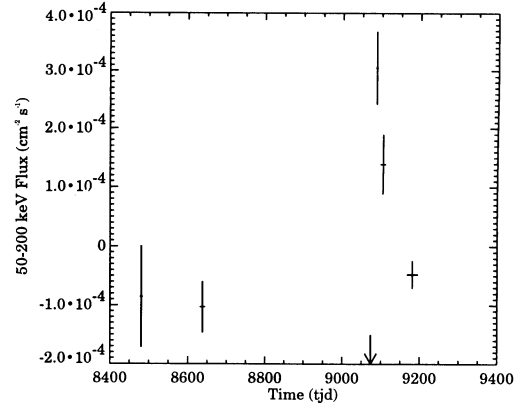


FIG. 4.—The hard X-ray flux measured by OSSE in five separate observations of the M81/M82 region. The outburst of SN 1993J is shown by the arrow.

SN 1993J just before and during the first OSSE detection. Both observed declining fluxes after that time, with approximate e -folding times of 86 days (Zimmermann et al. 1994) and 60 days (Wheeler & Filippenko 1994), respectively. The OSSE flux variations are, within the large uncertainties, consistent with these declines, as if from the same source. As described below the observed OSSE spectra extrapolate for thermal models, with large uncertainties, very close to the *ROSAT* (0.1–2.4 keV) and *ASCA* (1–10 keV) spectra at similar times. Nature could be so perverse as to cause another source to mimic what we might reasonably expect to be the spectrum and time variation of emission from SN 1993J, but we view that as less likely than that the emission is from SN 1993J.

Hard X-ray emission of this intensity was not anticipated. It is almost certainly not from scattered γ -rays from radioactivity. The optical light curve has quite well revealed the mass of ^{56}Co present, and even if it was mixed through the entire ejecta, the hard X-ray flux from it is roughly a factor of 3 below the OSSE sensitivity in these observations, as are the γ -ray line fluxes (Woodsley et al. 1994). The observed spectrum is also significantly steeper than that of down-scattered line photons. The low-energy X-ray observations were quite naturally explained in terms of the reverse-shocked supernova ejecta (Suzuki et al. 1993; Chevalier & Fransson 1994), although a contribution from the shocked wind could also be present. The electron temperature we find, 10^9 K , is easily accounted for in the shocked wind for either relatively modest expansion velocities (10^4 km s^{-1}) with equal electron and ion temperatures (Fransson 1984), or for higher ejecta velocities in non-equipartition solutions (Suzuki et al. 1993). However, all calculations indicate the ejecta free-free luminosity exceeds that of the lower density wind by at least an order of magnitude. We can check the possibility that both emission regions are seen by comparing the soft and hard X-ray spectra.

The extrapolation of OSSE spectra to keV energies is very uncertain. We show in Figure 2 as a dashed line the intensity/temperature combinations that extrapolate to the absorption-corrected luminosity observed from 0.1 to 2.4 keV by *ROSAT* (Zimmermann et al. 1994) during the OSSE observation. The center of the contours extrapolates right to the *ROSAT* data. All points to the upper left of the dashed line are allowed in the sense that they do not exceed the observed soft flux. The dotted line shows models that extrapolate to the preliminary *ASCA* 1–10 keV flux (Tanaka 1993).

Although a power-law model also fits the OSSE data, the extrapolated best-fit power law greatly exceeds the observed

soft X-ray fluxes. Only very flat spectra, allowed at a few percent confidence, do not violate the soft X-ray constraint. Still a nonthermal source, or a partial contribution thereof, cannot be ruled out by the OSSE data.

The simplest interpretation is that there is a single free-free emission region with kT_e in the range 50–100 keV. If this is the shocked wind, the required high emissivity demands an unusually high density, of order 10^9 cm^{-3} for pure hydrogen. This in turn implies a high progenitor mass-loss rate, $\geq 10^{-4} M_\odot \text{ yr}^{-1}$ for a constant spherically symmetric wind with a velocity of 10 km s^{-1} . If the emission seen by OSSE is from the forward shock, there is little room left for a softer component from the reverse-shocked ejecta between the low-energy X-ray observations and the extrapolation from OSSE data. Also, with the high temperature and relatively high optical depth of the shocked wind, the power-law spectrum from Comptonization of photospheric photons would extend into the soft X-ray range (Fransson 1984). This is apparently not observed. We speculate that high-density clumps in the circumstellar matter could possibly avoid some of these problems.

Alternatively, the single emission region observed could be the shocked ejecta, but with an unusually high temperature. The favored model of Suzuki et al. (1993) has initial ejecta velocity of $5 \times 10^4 \text{ km s}^{-1}$ and gives a shocked ejecta temperature of $kT_e = 25 \text{ keV}$. To explain the OSSE data, the temperature and free-free luminosity have to be increased by factors 2–4 over this already rather extreme model. This could be achieved by some combination of increased velocity, shallower ejecta density gradient, and lower ejecta/wind density contrast. Any such model must also be tested against many other related constraints (Fransson, Lundqvist, & Chevalier 1994)

such as from the radio and optical light curves and models of the stellar atmosphere.

5. SUMMARY

For the first time a supernova has been detected in $> 50 \text{ keV}$ hard X-rays soon after outburst. This emission was observed to decline on a timescale of several weeks. If thermal in nature, the temperature was initially $T \approx 10^9 \text{ K}$. A contribution of a non-thermal source cannot be excluded. The observed emission probably arose from the interaction of the supernova ejecta with circumstellar material. The hard X-ray luminosity 10–15 days after outburst, $\approx 5 \times 10^{40} \text{ ergs s}^{-1}$ from 50 to 150 keV, dominates the observed luminosity of the interaction region. It is much larger than was anticipated prior to the event and larger than predicted by models designed to explain the observed $< 10 \text{ keV}$ X-ray emission. The $> 50 \text{ keV}$ emission might be bremsstrahlung from either the shocked presupernova wind or the reverse-shocked supernova ejecta. The former can easily have the requisite high electron temperature (10^9 K) but was not thought to be dense enough to give high enough luminosity, and there can be additionally very little softer emission from the latter without violating soft X-ray observations. For the ejecta itself to give the observed hard X-rays, rather extreme models with high expansion velocity are required. Understanding these and other observations of SN 1993J will ultimately lead to a detailed description of the structure of the presupernova star and its wind, and the energy of the explosion.

This work was supported by NASA grant DPR S-10987C.

REFERENCES

- Bhattacharya, D., et al. 1994, ApJ, in press
 Canizares, C. R., Kriss, G. A., & Feigelson, E. D. 1982, ApJ, 253, L17
 Chevalier, R. A. 1982, ApJ, 259, 302
 Chevalier, R. A., & Fransson, C. 1994, ApJ, 420, 268
 Dotani, T., Hayashida, K., Inoue, H., Itoh, M., Koyama, K., Makino, F., & Mitsuda, K. 1987, Nature, 330, 230
 Filippenko, A. V., Matheson, T., & Ho, L. C. 1993, ApJ, 415, L103
 Fransson, C. 1984, A&A, 133, 264
 Fransson, C., Lundqvist, P., & Chevalier, R. A. 1994, preprint
 Freedman, W. L., et al. 1994, ApJ, 427, 628
 Hoflich, P., Langer, N., & Duschinger, M. 1993, A&A, 275, L29
 Johnson, W. N., et al. 1993, ApJS, 86, 693
 Matz, S. M., Share, G. H., Leising, M. D., Chupp, E. L., Vestrand, W. T., Purcell, W. R., Strickman, M. S., & Reppin, C. 1988, Nature, 331, 416
 McKee, C. F. 1974, ApJ, 188, 335
 Nomoto, K., Suzuki, T., Shigeyama, T., Kumagai, S., Yamaoka, H., & Saio, H. 1993, Nature, 364, 507
 Phillips, J. A., & Kulkarni, S. R. 1993, IAU Circ., 5775, 1
 Podsiadlowski, P., Hsu, J. L., Joss, P. C., & Ross, R. R. 1993, Nature, 364, 509
 Pooley, G. G., & Green, D. A. 1993, IAU Circ., 5773, 1
 Schmidt, B. P., et al. 1993, Nature, 364, 600
 Sunyaev, R., et al. 1987, Nature, 330, 227
 Suzuki, T., Kumagai, S., Shigeyama, T., Nomoto, K., Yamaoka, H., & Saio, H. 1993, ApJ, 419, L73
 Swartz, D. A., Clocchiatti, A., Benjamin, R., Lester, D. F., & Wheeler, J. C. 1993, Nature, 365, 232
 Tanaka, Y. 1993, IAU Circ., 5753, 1
 Van Dyk, S. D., et al. 1993, BAAS, 25, 1244
 Wheeler, J. C., et al. 1993, ApJ, 417, L71
 Wheeler, J. C., & Filippenko, A. V. 1994, in Supernovae and Supernova Remnants, ed. R. McCray (Cambridge: Cambridge Univ. Press), in press
 Woosley, S. E., Eastman, R. G., Weaver, T. A., & Pinto, P. A. 1994, ApJ, 429, 300
 Zimmermann, H.-U., et al. 1994, Nature, 367, 621